NASA/TM—2000-210349

Raman Study of Uncoated and p-BN/SiC-Coated Hi-Nicalon Fiber-Reinforced Celsian Matrix Composites

Part 1: Distribution and Nanostructure of Different Phases

Gwénaël Gouadec
CNRS and ONERA, France

Philippe Colomban
CNRS, France

Narottam P. Bansal
Glenn Research Center, Cleveland, Ohio

National Aeronautics and
Space Administration

Glenn Research Center

August 2000

Trade names or manufacturers' names are used in this report for identification only. This usage does not constitute an official endorsement, either expressed or implied, by the National Aeronautics and Space Administration.

Available from

NASA Center for Aerospace Information
7121 Standard Drive
Hanover, MD 21076
Price Code: A03

National Technical Information Service
5285 Port Royal Road
Springfield, VA 22100
Price Code: A03

RAMAN STUDY OF UNCOATED AND p-BN/SiC-COATED Hi-NICALON FIBER-REINFORCED CELSIAN MATRIX COMPOSITES
PART 1: DISTRIBUTION AND NANOSTRUCTURE OF DIFFERENT PHASES

Gwénaël Gouadec[1,2]
CNRS and ONERA
France

Philippe Colomban[1]
CNRS
France

Narottam P. Bansal
National Aeronautics and Space Administration
Glenn Research Center
Cleveland, Ohio 44135

ABSTRACT

Hi-Nicalon fiber reinforced celsian matrix composites were characterized by Raman spectroscopy and imaging, using several laser wavelengths. Composite #1 is reinforced by as-received fibers while coatings of p-BN and SiC protect the fibers in composite #2. The matrix contains traces of the hexagonal phase of celsian, which is concentrated in the neighborhood of fibers in composite #1. Some free silicon was evident in the coating of composite #2 which might involve a {BN + SiC → BNC + Si} "reaction" at the p-BN/SiC interface. Careful analysis of C-C peaks revealed no abnormal degradation of the fiber core in the composites.

INTRODUCTION

Ceramic fiber-reinforced ceramic matrix composites (CMCs) exhibit a number of remarkable properties including light weight, refractoriness and chemical inertness. Moreover, their ability to retain good mechanical performance (high tensile strength and modulus, large fracture energy, and damage tolerance) at elevated temperatures, including in corrosive or oxidizing atmospheres, has driven the aircraft and space industries to try to incorporate them in rockets and turbine engines. SiC/celsian composites, for instance, are anticipated to withstand 1500°C in use conditions.[1] Indeed, SiC fibers exhibit good oxidation and creep resistance, up to ~1300°C for the Hi-Nicalon grade,[2] or even more for the new generation of fibers.[3] As for celsian, a barium aluminosilicate (BAS), not only is it refractory (melting point ~1760°C[4]), but it is also oxidation/corrosion resistant[5] and has rather low thermal expansion.[4]

Composites are heterogeneous; thus there is a need for microscopic, *in-situ*, identification and characterization of the phases. Raman micro-spectroscopy is particularly well suited for these purposes, and might become a "routine" method for composites analysis. This technique is sensitive to the chemical bonds (stretching and bending modes) as well as their relative organization (vibrational and external modes) and allows analysis whatever the state of

[1]Laboratoire Dynamique-Interactions-Réactivité (LADIR), UMR7075 - CNRS & Université Pierre et Marie Curie, Thiais, Val de Marne, 94320, France
[2]Département Matériaux & Systèmes Composites (DMSC), Office National d'Etudes et de Recherches Aérospatiales (ONERA), Chatillon, Hauts de Seine, 92322, France

polymorphism or crystallinity of the compounds.[6,7] Besides, Raman spectra can be used to evaluate the residual stress arising from the coexistence of phases having different coefficients of thermal expansion (α).[6-8] The knowledge of residual stress is helpful in assessing the reliability of composites. But the models for life prediction do not account for matrix crystallization[9], which is likely to occur at elevated temperatures required for CMCs consolidation.

In the first part of the paper, we use Raman micro-spectroscopy to locate and identify various phases in celsian matrix composites reinforced by uncoated or p-BN/SiC-coated Hi-Nicalon fibers. Results will be compared to macroscopic spectra, to see if the latter are sufficient to characterize the different samples. BN (nominal thickness 0.6μm) is intended to improve the mechanical behavior, but it is still reactive with the matrix and has to be protected with a SiC over-layer (~0.25μm).[10-12] Celsian is found in several forms, usually a monoclinic tectosilicate (3D-feldspar network), or a hexagonal diphyllosilicate (layered network). The knowledge of monoclinic celsian (MC) and hexagonal celsian (HC) preferential location will be of prime interest, knowing that α_{HC} is higher than α_{MC},[13] because of lower density of HC and layered structure. α varies over a wide range depending on the Si/Al ordering in the slabs, the barium stoichiometry and also the synthesis and annealing history.[14]

In a separate later paper, part 2,[15] the fiber stress state as well as the influence of the double coating will be assessed experimentally.

EXPERIMENTAL PROCEDURE

RAMAN EQUIPMENT

All Raman spectra were recorded with a "XY" spectrograph (Dilor, France) equipped with a double monochromator filter and a back-illuminated liquid nitrogen-cooled 2000 x 800 pixel CCD detector (Spex, a division of the Jobin-Yvon company, France). The spectra could be recorded either in "macro-configuration" (laser impact about 100-300 μm diameter) or, alternatively, in "micro-configuration" after focusing through a magnifying objective (impact reduced to 1μm diameter). The source, an "Innova 70" Argon-Krypton laser (Coherent, USA) permitted working with blue (457.9 and 488nm), green (514.5 and 530.9nm) or red (647.1nm) exciting lines. A motorized X-Y displacement table was used to map the surface of the samples (step by step recording). With the 1800 lines per mm grating used in the monochromator, the wavenumber window ranged typically from 400 cm^{-1} (red laser) to 1000 cm^{-1} (blue laser). Larger windows required merging separate recordings. For the standard 120 μm opening of the slits, the resolutions were approximately 0.25 and 0.55 cm^{-1} in red and blue, respectively. Typical power levels used were 1 or 2 mW (on the sample).

COMPOSITE FABRICATION

Composites were unidirectional with 12 plies containing either (composite #1, fiber volume fraction V_f = 35%) flame-desized Hi-Nicalon fibers or (composite #2, V_f = 28%) Hi-Nicalon fibers that had been coated by chemical vapor deposition (CVD) with a layer of pyrolytic boron nitride (p-BN; deposition temperature 1400°C, thickness ~0.6μm) and an outer layer of SiC (deposition temperature ~1200-1300°C, thickness ~0.3 μm).[10-12] Fiber-reinforced composites were fabricated as described elsewhere.[10,11] The matrix was consolidated by hot pressing. A mixture of $BaCO_3$, $SrCO_3$, Al_2O_3 and SiO_2 powders, in the right proportions to give a $(0.75Ba/0.25Sr)Al_2Si_2O_8$ final composition[10,11,16] was first calcined and then used as a powdered precursor to the matrix.

SAMPLE PREPARATION FOR RAMAN ANALYSIS

Before examination, samples were polished with abrasive paper and diamond paste (1μm). Due to the low transparency of the celsian (≤20μm), no fiber spectra could be recorded through the matrix and most mappings were performed on sections polished perpendicular to the fiber direction (cross sectional mapping). One piece of composite #2 was polished with an approximate 15° θ angle between the fiber plies and the surface, in order to map an "apparent" interphase thickness four times higher than the "true" one ($\sin^{-1}\left(\frac{\pi}{12}\right)$ = 3.86).

SPECTRA TREATMENT

The procedure for the fitting of the carbon spectra has been discussed elsewhere.[17] As for celsian spectra, their treatment started with the subtraction of a linear baseline attached to the limits of a restricted working window (380-445 cm^{-1}), followed by a 4-band fitting (Labspec software, Dilor, France). The bands were characterized by their half height width (w) and their form, which could be changed continuously from purely Gaussian to purely Lorentzian by a "Gauss proportion" g ($0<g<1$). w and g values were fixed for each band on the basis of preliminary testing. The main band of the MC phase (508 cm^{-1}) was fitted separately with unset g and w values.

RESULTS

MATRIX EXAMINATION: CELSIAN POLYMORPHISM AND ITS LOCATION

Figure 1(a) shows matrix spectra of composites #1 (uncoated fibers) and #2 (coated fibers) with the spectrum of a fiber-free monolith, for comparison. The bands could be attributed by comparison with spectra recorded on pure HC and (Li-doped) pure MC monoliths.[5] Due to MC lower symmetry, its spectrum has many more lines than that of HC. From the molecular point of view, the main band for both phases originates from the ν_2 bending of SiO_4 tetrahedra,[5] which are either isolated (HC), or linked by oxygen ions (MC). This is usually the strongest mode in structures consisting of connected SiO_4 rings and in tectosilicates in general. This band is located at 406cm^{-1} (g = 0.80; w = 5.00 cm^{-1}) in HC and 508 cm^{-1} in MC. Figures 1(b) and 1(c) present two spectra series recorded as a function of the distance to the nearest fiber in composite #1 and composite #2, respectively. The fitting in the 380-440cm^{-1} range led to mean values of 392 cm^{-1} (g = 0.45; w= 4.50 cm^{-1}), 408.5 cm^{-1} (g= 0.55; w= 8.50 cm^{-1}) and 428 cm^{-1} (g= 0.15; w= 6.50 cm^{-1}) for the MC peaks. Figure 1(d) shows the I_{406}/I_{508} and I_{406}/I_{428} ratios calculated from a fitted series of spectra recorded on another area of composite #2 than is shown in figure 1(c), with another laser line.

THE INTERPHASE MATERIALS IN COMPOSITE #2

Figure 2 shows a large coating thickness variation from fiber to fiber, especially for the SiC layer. Some SiC layers were also broken.

***BN coating*:** Figure 3(b) compares Raman spectra recorded on some BN layers of composite #2. The spectra of the cubic (c-BN[18]) and hexagonal (h-BN) crystalline forms of boron nitride are given for comparison in figure 3(a). The carbon spectrum recorded on the core of a fiber of composite #2 is also given in figure 3(c). Although c-BN[19] and h-BN have medium Raman efficiencies, figure 3(b) exhibits a huge signal scattering, protruding from a wide background. The 457.9nm-excited spectra are even an order of magnitude more intense than the carbon spectrum of figure 3(c), recorded under the same conditions. Carbon being

resonant, we might conclude the BN coating is also resonant and has a huge electronic absorption in the visible range, but this will be discussed further. Resonance would explain why spectra change in figure 3(b) according to the wavelength. We also observed changes according to the area under examination and there must be strong chemical/structural heterogeneity at the microscopic scale in the BN layers. Yet, BN coating scattering allowed for easy imaging, as shown in figure 4(b). It is based on spectra recorded for each point in the optical micrograph of figure 4(a). The BN layers were easily located based on the 1s peaks.

SiC overcoating: The mapping of figure 5(b) was performed on the sample of composite #2 polished at a θ angle of ~15°. The distance separating consecutive recordings was 1μm, but would correspond to 0.26 μm for a "right angle" scanning of the SiC layer (θ = 90°). Figure 5(a) gives spectra representative of what was recorded elsewhere in composite #2.

SiC structures are formed by alternating layers of Si and C atoms. Two consecutive layers form a "bilayer" which is named "h" if it is deduced from the one below by a simple translation. If not, when an additional 180° rotation (around the Si-C bonds linking the bilayers) is necessary to get the superposition, then the bilayer is named "k". The "k-only" stacking is the reference structure of cubic symmetry (3C-SiC in Ramsdell notation[20]). Any other definite stacking sequence defines a peculiar structure and this is called polytypism.[21] More than 130 polytypes of SiC have been reported.[22] They have either hexagonal or rhombohedral lattice symmetry and are named NH or NR (Ramsdell notation), where N is the number of bilayers in the unit cell.[23] The peaks that protrude from a continuous background in figures 5(a) and 5(b) indicate a dominating contribution of one or several polytypes. These peaks were systematically detected, but figure 5(a) shows great discrepancies in their relative intensities. The "main" peak is centered at 796 cm^{-1}. Other peaks are located around 765, 785.5 and 966 cm^{-1}, with a weaker feature around 702 cm^{-1}.

In addition, the presence of a "free" silicon phase (ν ~ 520 cm^{-1}) is obvious in figure 5, but was not systematically analyzed. Two unidentified lines of approximately 10 cm^{-1} half-height widths were also detected in some instances around 1017 and 1047 cm^{-1}.

THE FIBERS

Figure 6(a) presents two carbon spectra recorded on a polished section of composite #1 with the 514.5 cm^{-1} line; one in "macro-configuration (simultaneous analysis of tens of fibers), the other one in "micro-configuration" (single fiber core analysis). Figure 6(b) shows analogous "micro-configuration" spectra recorded with three visible wavelengths (λ). Wavenumber and intensity changes like those observed as a function of λ are characteristic of a "resonance" phenomenon.[24] As a matter of fact, while SiC is the main phase in the Hi-Nicalon fiber (C:Si atomic ratio is about 1.4[25]), SiC is not detected at all.[26] Even in the latest nearly stoichiometric grades (C:Si ~1.05 in the Hi-S[27] and UF[28] fibers, 1.08 in the SA grade[29]), the carbon spectrum remains more intense than the SiC signal. Figure 7 illustrates the mean spectral parameters of the Hi-Nicalon fibers measured at different stages of the process, from the reception to the finished composite. The extracted fibers used as "reference" fibers were taken from composite #2 after matrix crushing in an agate mortar. Such fiber extraction could not be achieved in the case of composite #1, due to fiber strength degradation from mechanical damage during composite processing[10] and/or the nature of the interface. Figures 4(c) and 4(d) present the same kind of analysis as in figures 4(a) and 4(b), but were performed on composite #1. In this case, the resonance of C-C bonds made fiber imaging quite easy.

DISCUSSION

THE FIBER SPECTRA AND FIBER DEGRADATION

First band assignments in disordered carbons date back to the early seventies,[30] but the subject is still being discussed. Pure diamond and graphite having sharp peaks at 1331 and 1581cm^{-1}, respectively, the first temptation was to assign the main two bands of amorphous carbons to diamond-like and graphite-like entities. This is the reason why the bands were named D and G (see figure 6).[31] There is actually no doubt that the G band ensues from the stretching mode of C_{sp^2}- C_{sp^2} bonds (E_{2g} symmetry in graphite crystals). As for D, its attribution is complicated by its strong resonant character, evidenced by a high dependence of the intensity and position (# 50 cm^{-1}/eV) on wavelength[32] as well as an enhancement of the "$2\times\nu_D$" and "$\nu_D+\nu_D$" harmonics under blue excitation.[33,34] As a matter of fact, resonance excites the bonds and makes the usual "structural approach" inappropriate. Because the diamond cross-section is much lower than that of graphite (9.1×10^{-7} and 5×10^{-5} cm^{-1}/sr, respectively[35]) a weak C_{sp^3}-C_{sp^3} stretching mode should be expected. C_{sp^2}-C_{sp^3} bonds must concentrate at carbon crystallite grain boundaries, in contact with the favorably sp^3-hybridized Si and C atoms of the SiC fiber network. The density of these bonds is proportional to L^2, where L represents the mean size of graphitic moieties, while C_{sp^2}-C_{sp^2} density should obey L^3 dependence. As a matter of fact, the intensity ratio I_D/I_G is proportional to L^{-1} [30] which not only allows for crystal size analysis,[36] but also supports an assignment of D to the C_{sp^2}-C_{sp^3} stretching mode.[37] Moreover, D falls in the range of bands detected in new forms of carbonaceous species like C_{70} and tubular fullerenes where angled "C_{sp^2}-C_{sp^3}" bonds dominate the structure.[26] However, in disordered diamond, the 1331cm^{-1} single peak of "C_{sp^3}-C_{sp^3}" single bonds, which must be abundant in SiC fibers (dominated by sp^3 hybridization), is broadened and its wavenumber increases up to 1340 cm^{-1}.[38] We detect frequencies as high as 1355cm^{-1}, which must indicate a high dispersion in length and angles. Some C_{sp^3}-C_{sp^3} contribution to the low wavenumber side is also possible since D is abnormally large for a "single band". A component was even clearly evidenced in the case of the NLM-Nicalon fiber observed under red excitation.[6] In conclusion, we think the D band should be attributed to vibrations involving "C_{sp^3}-$C_{sp^3}/_{sp^2}$" bonds. But $\sigma\rightarrow\sigma^*$ lowest electronic transitions in graphite have gaps in the UV range and only $\pi\rightarrow\pi^*$ transitions could explain resonance for visible range laser excitations.[32] It has been proposed that D is a mode of graphite vibration density of state ("VDOS"), after "Brillouin zone folding", very common in highly disordered materials, and selective enhancement by the $\pi\rightarrow\pi^*$ transition corresponding to each visible line.

The so-called "graphite-like" band is in fact a doublet, well resolved in recent grades[39] of fibers. G band at #1595 cm^{-1} has a shoulder, around 1625 cm^{-1}, which was named D' since it behaves in many ways like D.[40] There is a problem in fitting such overlapping contributions (see for example Wagner *et al*[41]). Besides, there is a disturbing contribution of carbon bonded to heteroatoms.[36,42] Lastly, D' "resonance" disturbs G. The carbon atoms contributing to the D band should be better incorporated to the SiC network than those corresponding to G, in the bulk of graphitic entities.

Figure 6(a) underlines that a spectrum recorded in macro configuration looks very similar to the spectra recorded on single fiber under a microscope. We are in a favorable case where the spectrum is not disturbed by contributions from other phases (like BN in composite #2) and carbon bandwidths could be used to characterize the repartition of the different configurations. A microanalysis would probably remain necessary to study the influence of environment (distance and number of closest fibers, contact with a neighboring fiber, proximity of a fiber crack or damaged parts of the matrix...). Figure 7 shows that spectra are hardly altered when the coatings are applied. A more interesting finding for composite #1

which needs to be checked is that the bandwidth, hence the chemical state[6], of fibers extracted from the composite has, within the measurement error, the same value as for the pristine fibers. No significant degradation has occurred, but the slight band narrowing shows, however, that the structure has somewhat evolved and that the stability limit is reached, as confirmed by "reference curves" for freestanding fibers.[6,26] A specific surface study would probably be useful.

MATRIX POLYMORPHISM AND ITS ORIGIN

Because the MC phase is thermodynamically stable from room temperature to 1590°C, one will want this phase to predominate for thermostructural applications of barium aluminosilicates. Yet, HC usually forms first and most synthesis routes lead to MC/HC mixtures.[5] Although long time thermal annealing (>1500°C, > 20hrs) allows nearly full HC to MC conversion,[43,44] it must be avoided to prevent degradation of fiber properties and, mostly, to avoid volume changes and subsequent micro cracking of the matrix. The solution for lower temperature (T<1200°C) MC synthesis is sol-gel processing,[13,14] but helping the formation of MC is also possible by adding alkali/alkaline-earth mineralizers like Li^+ [45] (BLAS) or, in our case, Sr^{2+} (BSAS). As a matter of fact, figure 1 shows that the BSAS matrix contains mere traces of the HC phase. Its main band (around 406 cm^{-1}) is indeed hardly visible in spite of a very high Raman efficiency compared to that of MC.[5,14] X-rays patterns did not detect any HC in the hot pressed monolith, nor in fiber-reinforced composites. Figure 1(a) suggests that the HC signal vanishes when fibers are incorporated in the celsian matrix. Knowing that a migration of Ba^{2+} ions has been reported from Li-enriched celsian matrices to reinforcing fibers of the NLM202 grade,[5,13] one would expect the same phenomenon to also occur for the Ba-free Hi-Nicalon fibers reinforcing composites#1 and 2. This would result in a matrix Ba deficit, which has been proposed as an explanation for HC formation.[46-48] Yet, scanning microprobe analysis did not detect Ba/Sr diffusion from the matrix into the uncoated fibers (unpublished results). Due to its lamellar structure, HC should cleave easily and might play an important role in the mechanical properties of the composite if it concentrated as a second phase in the neighborhood of fibers, as figure 1(b) suggests in the case of composite #1 (uncoated fibers). The fibers of composite #2 are covered by a p-BN/SiC interphase which is still Ba-free. Figure 1(c) does not show any preferential concentration of HC around the fibers of composite #2; rather, tiny HC domains form from place to place, even in fiber-free regions. Microscopy and EDS analysis revealed a bright phase deficient in Al and Ba.[10,16] It might correspond to HC. In fact, due to the background rising as a function of decreasing distance to the nearest fiber, we did not get information closer than 6 μm from each coated fiber in composite #2, but the HC proportion did not seem to be increasing. Other composite #2 probings confirmed this trend. The protective p-BN/SiC coating probably hinders the Ba migration as expected from composite #1 behavior.

Since both the 508 cm^{-1} and 406 cm^{-1} peaks correspond to the bending mode of SiO_4 tetrahedra in the frameworks (ν_2), their ratio could be used to estimate MC and HC relative concentrations. Figure 1(d) shows an almost perfect correlation exists between the ratios L_{406}/I_{508} and L_{406}/L_{428}. The latter ratio might be able to measure very small HC concentrations, on the basis of a calibration that is still to be done. Besides, the good agreement of figures 1(c) and 1(d) shows any region is representative of the whole sample. Note that our fitting procedure takes a 410 cm^{-1} MC contribution into account, which explains how the ratio occasionally vanishes. One must assume HC is totally absent from the corresponding points.

INTERPHASE ANALYSIS IN COMPOSITE #2

Nature of the p-BN coating: BN was used as a compliant layer for protecting the fibers. In h-BN (graphite-like structure), only the E_{2g} lines are Raman active. Points at 52 cm^{-1} (42 cm^{-1} in graphite) and 1366 cm^{-1} (1581) were observed with the 514 nm line.[49,50] A value of 1381 cm^{-1} was found with the same line in the case of an h-BN film.[19] As for c-BN (diamond-like "blend" structure), it has TO and LO Raman modes at 1056 and 1306 cm^{-1} (These modes are degenerate at 1333 cm^{-1} in diamond).[50,51] In the specific case of composite #2 interphase, the high level of scattering made it difficult to analyze but the vertical lines drawn on figure 3(b) underline characteristic components we found at 1230 and 1366 cm^{-1} for blue and green excitations. These features were also present on a spectrum we recorded with a red laser line (λ=647.1nm), with an additional feature around 1320 cm^{-1}. Our spectra are very similar to the spectra recorded between c-BN and h-BN domains by Eremets et al, which also exhibited a wavelength dependency.[52] All the features being present whatever the excitation, they correspond to definite vibrational modes with contributions of other types superimposing (fluorescence?). If the 1365.8cm^{-1} band was due to carbon, it would shift according to the wavelength. Rather, we clearly have a h-BN contribution, but the 1230 cm^{-1} feature might correspond to the LO mode of c-BN, which has already been detected around 1260 cm^{-1} in nanoprecipitates,[19] due to strain-induced bond length changes or the presence of defects such as vacancies or heteroatoms.

The high scattering we observed from our BN layers has already been reported for h-BN powdered samples.[49] Since the h-BN bandgap is higher (>5eV) than the visible laser's energy, a resonance-based explanation must involve a BNC solid solution formation, with electronic absorption in the visible range. Harmonics should be visible in the 2650-2750 cm^{-1} region in case of resonance. We could not detect them, but the harmonics are usually weak. As for the background, it must originate from fluorescence due to cracks or impurities trapped in the macro/micro-porosity. We sometimes observed a background reduction after a long time laser illumination and contamination is thus likely. Some "free" carbon is obviously detected in figure 3(b) (vertical line at 1590 cm^{-1}) and we infer diffusion in the BN network. It must however be noted that boron carbides can give significant Raman intensity in the range 1200-1600cm^{-1}.[53] As for C-N bonds, their vibrations are in the ranges 1200-1250 cm^{-1} for single bond[54] and 1470-1520cm^{-1} for double bond.[55] They are usually associated with the formation of chromophore species or even with electronic delocalization, making them absorbent in the visible/UV domain. In structures including atoms of very close masses such as B, N and C, vibrational coupling between the different stretching modes systematically occurs and a simple "molecular approach" is inappropriate. An XPS analysis in selective sections of the BN layers is required for a more complete discussion. But we have trends similar to carbon nanoprecipitates, with a major contribution of "E_{2g}" modes (hexagonal planes) and a size/disorder-activated cubic-like contribution.

The SiC over-coating: The mapping of figure 5(b) indicates "free" silicon is present in the SiC deposit surrounding the fibers of composite #2 (ν ~520 cm^{-1}). However, we found other SiC ring sections which did not show any silicon signal. Detecting silicon is in agreement with previous scanning auger microscopy studies that found a 300nm Si-rich SiC zone.[12,56] Figure 8 presents the raw peak intensities that were measured for all the phases detected in figure 5(b). The silicon profile indicates a preferential location at the very p-BN/SiC interface, where intensity would be at maximum if the laser was not already somewhat overlapping the BN layer. EELS analysis of a boron-doped SiC showed presence of boron at SiC grain boundaries.[57] With boron replacing silicon atoms, it is therefore not surprising to find "free" silicon in the region in contact with the BN layer. This might result

from (i) the existence of a transitional CVD atmosphere when BN precursors are replaced by the SiC precursors or (ii) a SiC/BN interdiffusion during the hot pressing stage. The steady vanishing of the silicon signal suggests diffusion across SiC towards the matrix, where silicon is no longer detected. Si depletion is supposed to occur at 1600°C only in "bare" Hi-Nicalon fibers,[2] but a reaction with the matrix is possible. It looks like there is a {BN + SiC → BNC + Si} reaction taking place, which would account for BN signal enhancement (a BNC solid solution would have a high electronic absorption). The only way to know what does occur would be to analyze a fiber as it is received after the BN/SiC deposition. The observation would require embedding in nickel for the samples to be polished correctly (electrochemical deposit, see Gouadec et al[58] in the case of a Textron SCS6 fiber).

The SiC layer phase was intended to be crystalline and act as a diffusion barrier.[11] Yet, the background on the spectra of figure 5 indicates a certain level of disorder, increasing on the matrix side with regard to the BN side (5(b)). As proposed by Karlin & Colomban,[26] such background results from a disorder-activated Brillouin zone folding which makes the whole VDOS contribute to the spectra. However, four peaks protrude from the background and indicate one polytype is dominant. Only in β-SiC are transverse optic modes, TO_1 and TO_2, degenerate. TO_1 points occur at 796 cm^{-1} whatever the polytype, but TO_2, a satellite line of lower intensity than TO_1 is shifted according to the percentage p (where $0<p<100$) of "h" layers in the polytype.[59] A 3.3 %/cm^{-1} dependency was found on the basis of data from Feldman *et al*[60] and Salvador & Sherman.[23] The 785.5 cm^{-1} peak should then correspond to the TO_2 mode of a p=34% polytype. The closest among the most common we have data on (4H[60], 6H[61,62], 8H[59], 15R[60,62], 21R[60], 27R[63], 33R[63]) is the 6H polytype (p=33%). It must be noted that 8H (p=25%) and 21R (p=28%) have their TO_2 peak in the same region,[64] but only 6H happens to have a mode at ~768 cm^{-1}, which we detect. Besides, 6H longitudinal optic (LO) mode is expected at the 966 cm^{-1} value we measured (972cm^{-1} in β-SiC). Two 6H acoustical (low energy) modes are expected at 140 and 150 cm^{-1} and we did find spectral features around 125 and 150 cm^{-1}. Given the background they protruded from, these modes might be considered the same. Then, the SiC nature is different in the SiC layer of composite#2 (6H-SiC) than in the fibers (x-rays studies evidenced β-SiC crystallites). This might result in a difference in Si/Ba exchange, which was suggested above as an explanation for HC formation.

On the BN side of the SiC coating, B-O vibrations might overlap with the TO/LO fingerprint of SiC. They appear at 807 cm^{-1} in pure B_2O_3, but can be detected from 770 to 885 cm^{-1} in B_2O_3-based structures.[65] Lastly, the presence of a 702cm^{-1} component in SiC compounds has, to our knowledge, never been reported before.

SUMMARY

Raman spectroscopy is useful for the physical and chemical analysis of multiphase materials like composites. Its high spatial resolution allowed us to investigate phenomena taking place in a thin BN coating: a BNC phase (solid solution?) develops as a result of C/BN interdissolution and a pseudo reaction between BN and the SiC overlayer releases some silicon. The Raman scattering efficiency of hexacelsian makes it far more detectable by Raman spectroscopy than by X-rays. Hexacelsian formation seems to be favored near the fibers; this might result from Ba/Sr atoms diffusing into the fibers or nucleating effect of elements at the fiber surface. The fibers do not seem to degrade chemically during composite fabrication, but their spectra depend on the residual stress, which will be investigated in part 2.

REFERENCES

[1]N.P. Bansal, "Influence of Fiber Volume Fraction on Mechanical Behavior of CVD SiC Fiber/$SrAl_2Si_2O_8$ Glass-Ceramic Matrix Composites," *J. Adv. Mater.*, **28** [1], 48-58 (1996).

[2]G. Chollon, R. Pailler, R. Naslain and P. Olry, "Correlation Between Microstructure and Mechanical Behavior at High Temperatures of a SiC Fiber with a Low Oxygen Content (Hi-Nicalon)," *J. Mater. Sci.*, **32**, 1133-1147, (1997).

[3]T. Ishikawa, Y. Kohtoku, K. Kumagawa, T. Yamamura and T. Nagasawa, "High-Strength Alkali-Resistant Sintered SiC Fiber Stable to 2,200°C," *Nature*, **391** [6669], 773-775 (1998).

[4]X.-D. Zhang, K.H. Sandhage and H.L. Fraser, "Synthesis of $BaAl_2Si_2O_8$ from Solid Ba-Al-Al_2O_3-SiO_2 Precursors: PartIII; the Structure of $BaAl_2Si_2O_8$ Formed by Annealing at <650°C and at 1650°C," *J. Mater. Res.*, **13** [11], 3122-3133 (1998).

[5]T. Scanu, J. Guglielmi and Ph. Colomban, "Ion Exchange and Hot Corrosion of Ceramic Composites Matrices: a Vibrational and Microstructural Study," *Solid State Ionics*, **70/71**, 109-120 (1994).

[6]Ph. Colomban, "Raman Microspectrometry and Imaging of Ceramic Fibers in CMCs and MMCs," in *Advances in Ceramic Matrix Composites V*, N.P. Bansal, J.P. Singh, and E. Ustundag, Editors; Am. Ceram. Soc (Westerville, OH, U.S.A.) pp 517-540 (2000).

[7]Ph. Colomban, "Stress- and Nanostructure-Imaging of Ceramic Fibers and Abradable Thermal Barrier Coatings by Raman Microspectrometry: State of the Art and Perspectives," *Ceram. Eng. Sci. Proc.*, **21** (2000).

[8]Ph. Colomban and J. Corset, "Special Issue on Raman (Micro)Spectrometry and Materials Science," *J. Raman. Spectrosc.*, **30** [10], 861-947 (1999).

[9]X. Yang and R.J. Young, "Model Ceramic Fiber-Reinforced Glass Composites: Residual Thermal Stresses," *Composites*, **25** [7], 488-493 (1994).

[10]N.P. Bansal and J.I. Eldridge, "Hi-Nicalon Fiber-Reinforced Celsian Matrix Composites: Influence of Interface Modification," *J. Mater. Res.*, **13** [6], 1530-1537 (1998).

[11]N.P. Bansal, "Strong and Tough Hi-Nicalon-Fiber-Reinforced Celsian Matrix Composites," *J. Am. Ceram. Soc.*, **80** [9], 2407-2409 (1997).

[12]N.P. Bansal, "Tensile Strength and Microstructure of Hi-Nicalon Fibers Extracted from Celsian Matrix Composites," in *Advances in Ceramic Matrix Composites IV*, J.P. Singh and N.P. Bansal, Editors ; Am. Ceram. Soc (Westerville, OH, U.S.A.) pp 3-16 (1999).

[13]Ph. Colomban and N. Lapous, "New Sol-Gel Matrices of Chemically Stable Composites of BAS, NAS and CAS," *Comp. Sci. Techn.*, **56**, 739-746 (1996).

[14]Ph. Colomban, H. Courret, F. Romain, G. Gouadec and D. Michel, "Sol-Gel Prepared Pure and Li-Doped Hexacelsian Polymorphs: An IR, Raman and Thermal Expansion Study of the β Phase Stabilization by Frozen Short-Range Disorder," *J. Am. Ceram. Soc (To be published).*

[15]G. Gouadec, Ph. Colomban and N.P. Bansal, "Raman Study of Uncoated and p-BN/SiC-Coated Hi-Nicalon Fiber Reinforced Celsian Matrix Composites, Part2: Residual Stress in the Fibers," *J. Am. Ceram. Soc. (submitted).*

[16]N.P. Bansal, "Solid State Synthesis and Properties of Monoclinic Celsian," *J. Mater. Sci.*, **33** [19], 4711-4715 (1998).

[17]G. Gouadec, S. Karlin and Ph. Colomban, "Raman Extensometry Study of NLM202 and Hi-Nicalon SiC Fibers," *Composites*, **29B**, 251-261 (1998).

[18]T. Werninghaus, J. Hahn, F. Richter and D.R.T. Zahn, "Raman Spectroscopy Investigation of Size Effects in Cubic Boron Nitride," *Appl. Phys. Lett.*, **70** [8], 958-960 (1997).

[19]A. Bonizzi, R. Checchetto, A. Miotello and P.M. Ossi, "Low-Temperature Deposition of Cubic Boron Nitride Thin Films," *Europhys. Lett.*, **44** [5], 627-633 (1998).

[20]L. Patrick, "Infrared Absorption in SiC Polytypes," *Phys. Rev.*, **167** [3], 809-813 (1968).

[21]W.J. Choyke and G. Pensl, "Physical Properties of SiC," *MRS Bull.*, **22** [3], 25-29 (1997).

[22]H. Okumura, E. Sakuma, J.H. Lee, H. Mukaida, S. Misawa, K. Endo and S. Yoshida, "Raman Scattering of SiC: Application to the Identification of Heteroepitaxy of SiC Polytypes," *J. Appl. Phys.*, **61** [3], 1134-1136 (1987).

[23]G. Salvador and W.F. Sherman, "Pressure Dependence of the Raman Phonon Spectrum in 6H-Silicon Carbide," *J. Molec. Struct.*, **247**, 373-384 (1991).

[24]W. Kiefer and M. Spiekermann, "Applications of Non-Classical Raman Spectroscopy : Resonance Raman, Surface Enhanced Raman, and Nonlinear Coherent Raman Spectroscopy," in *Infrared and Raman Spectroscopy. Methods and Applications*, B. Schrader Editor, VCH (Weinheim), pp 465-517 (1995).

[25]G. Chollon, R. Pailler and R. Naslain, "Structure, Composition and Mechanical Behavior at High Temperature of the Oxygen-Free Hi-Nicalon Fiber"; pp 299-304 in Proceedings of High temperature CMCs, N°2 (1995).

[26]S. Karlin and Ph. Colomban, "Raman Study of the Chemical and Thermal Degradation of As-Received and Sol-Gel Embedded Nicalon and Hi-Nicalon SiC Fibers Used in Ceramic Matrix Composites," *J. Raman Spectrosc.*, **28**, 219-228 (1997).

[27]M. Takeda, J. Sakamoto, A. Saeki, Y. Imai and H. Ichikawa, "High Performance Silicon Carbide Fiber Hi-Nicalon for CMCs," *Ceram. Eng. Sci. Proc.*, **16** [4], 37-44 (1995).

[28]M.D. Sacks and J.J. Brennan, "Silicon Carbide Fibers with Boron Nitride Coatings," *Ceram. Eng. Sci. Proc.*, **21** (2000).

[29]K. Kumagawa, H. Yamaoka, M. Shibuya and T. Yamamura, "Fabrication and Mechanical Properties of New Improved Si-M-C-(O) Tyranno Fiber," *Ceram. Eng. Sci. Proc.*, **19** [3], 65-72 (1998).

[30]F. Tuinstra and J.L. Koenig, "Characterization of Graphite Fiber Surfaces with Raman Spectroscopy," *Comp. Mater.*, **4**, 492 (1970).

[31]R. Vidano and D.B. Fischbach, "New Lines in the Raman Spectra of Carbons and Graphite," *J. Am. Ceram. Soc.*, **61** [1-2], 13-17 (1978).

[32]I. Pócsik, M. Hundhausen, M. Koós and L. Ley, "Origin of the D Peak in the Raman Spectrum of Microcrystalline Graphite," *J. Non Cryst. Solids*, **227-230**, 1083-1086 (1998).

[33]Y. Sato, M. Kamo and N. Setaka, "Raman Spectra of Carbons at 2600-3300 cm^{-1} Region," *Carbon*, **16**, 279-280 (1978).

[34]G. Gouadec and Ph. Colomban, "Raman Extensometry : Anharmonicity and Stress"; pp 759-766 in Proceedings of 11èmes Journées Nationales sur les Composites (JNC11)-Arcachon, France, Nov 18-20 (1998) ; Edited by AMAC (J. Lamon and D. Baptiste Editors).

[35]N. Wada and S.A. Solin, "Raman Efficiency Measurements of Graphite," *Physica*, **105B**, 353-356 (1981).

[36]M. Ramsteiner and J. Wagner, "Resonant Raman Scattering of Hydrogenated Amorphous Carbon: Evidence for π-Bonded Carbon Clusters," *Appl. Phys. Lett.*, **51** [17], 1355-1357 (1987).

[37]S. Rohmfeld, M. Hundhausen and L. Ley, "Raman Scattering in Polycrystalline 3C-SiC: Influence of Stacking Faults," *Phys. Rev.*, **B58** [15], 9858-9862 (1998).

[38]P.V. Huong, "Diamond and Diamond Films Studied by Raman Spectroscopy," *J. Molec. Struct.*, **292**, 81-88 (1993).

[39]G. Gouadec, J.-P. Forgerit, H. Mendil, K. Devivier and Ph. Colomban, "Extensométrie Raman de Fibres C et SiC: Choix des Conditions par Corrélation 2D (Raman Extensometry of C and SiC Fibers: Conditions Choice by 2D Correlation)"; in Proceedings of JNC12 (2000).

[40]T. Raphael, H.J. Gonzallez and C.I. Hernandez, "Observation of Splitting of the E_{2g} Mode and Two-Phonon Spectrum in Graphites," *Solid state Comm.*, **27**, 507-510 (1978).

[41]J. Wagner, M. Ramsteiner, C. Wild and P. Koidl, "Resonant Raman Scattering of Amorphous Carbon and Polycrystalline Diamond Films," *Phys. Rev.*, **B40** [3], 1817-24 (1989).

[42]M. Yoshikawa, G. Katagiri, H. Ishida, A. Ishitani and T. Akamatsu, "Raman Spectra of Diamond-Like Amorphous Carbon Films," *Solid State Comm.*, **66** [11], 1177-1180 (1988).

[43]D. Bahat, "Kinetic Study on the Hexacelsian-Celsian Phase Transformation," *J. Mater. Sci.*, **5**, 805-810 (1970).

[44]M.J. Hyatt and N.P. Bansal, "Crystal Growth Kinetics in $BaOAl_2O_32SiO_2$ and $SrOAl_2O_32SiO_2$ Glasses," *J. Mater. Sci.*, **31** [1], 172-184 (1996).

[45]M. Chen, W.E. Lee and P.F. James, "Preparation and Characterization of Alkoxide-Derived Celsian Glass-Ceramic," *J. Non-Cryst. Solids*, **130**, 322-325 (1991).

[46]R. Dimitrijevic, A. Kremenovic, V. Dondur, M. Tomasevic-Canovic and M. Mitrovic, "Thermally Induced Conversion of Sr-exchanged LTA- and FAU-Framework Zeolites. Synthesis, Characterization and Polymorphism of Ordered and Disordered $Sr_{1-x}Al_{2-2x}Si_{2+2x}O_8$ (x=0, 0.15) Diphyllosilicate and Feldspar Phase," *J. Phys. Chem.*, **B101**, 3931-3936 (1997).

[47]A. Kremenovic, P. Norby, R. Dimitrijevic and V. Dondur, "High Temperature Synchrotron Powder Diffraction Investigation of Thermal Expansion, Strain and Microstructure for the co-elastic α–β Hexacelsian Transition," *Phase Transition*, **68** [4], 587-607 (1998).

[48]V. Dondur, R. Dimitrijevic, A. Kremenovic, U.B. Mioc, R. Srejic and M. Tomasevic-Canovic, "Structural Characterization of Hexagonal $Ba_{1-x}Al_{2-2x}Si_{2+2x}O_8$ Phases Synthesized from Zeolith Precursors," in *Adv. Sci. Techn.*, P. Vincenzini Editor, Techna (Faenza), pp 687-694 (1995).

[49]R.J. Nemanich, S.A. Solin and R.M. Martin, "Light Scattering Study of Boron Nitride Microcrystals," *Phys. Rev.*, **B23** [12], 6348-6356 (1981).

[50]P.V. Huong, "Structural Studies of Diamond Films and Ultrahard Materials by Raman and Micro-Raman Spectroscopies," *Diamond and Related Materials*, **1**, 33-41 (1991).

[51]M. Yoshikawa, H. Ishida, A. Ishitani, T. Murakami, S. Koizumi and T. Inuzuka, "Study of Crystallographic Orientations in the Diamond Film on Cubic Boron Nitride Using Raman Microprobe," *Appl. Phys. Lett.*, **57** [5], 428-430 (1990).

[52]M.I. Eremets, K. Takemura, H. Yusa, D. Golberg, Y. Bando, V.D. Blank, Y. Sato and K. Watanabe, "Disordered State in First-Order Phase Transitions: Hexagonal-to-Cubic and Cubic-to-Hexagonal Transitions in Boron Nitride," *Phys. Rev.*, **B57** [10], 5655-5660 (1998).

[53]U. Kuhlmann and H. Werheit, "Improved Raman Effect Studies on Boron Carbide ($B_{4.3}C$)," *Phys. Stat. Sol.*, **B175**, 85-92 (1993).

[54]Y. Furakawa, T. Hara, Y. Hyodo, I. Harada, T. Nakajima and T. Kawagoe, "Vibrational Spectra and Structure of Polyaniline," *Macromolecules*, **21**, 1297-1305 (1988).

[55]S. Folch, A. Gruger, A. Regis and Ph. Colomban, "Optical and Vibrational Spectra of Sols/Solutions of Polyaniline : Water as a Secondary Dopant," *Synth. Metals*, **81**, 221-225 (1996).

[56]N.P. Bansal and J.I. Eldridge, "Effects of Fiber/Matrix Interface and its Composition on Mechanical Properties of Hi-Nicalon/Celsian Composites"; Paper N°147 in Proceedings of 12th Int. Conf. on Comp. Mater. (ICCM 12)-Paris, France, July 5-9 (1999).

[57]H. Gu, Y. Shinoda and F. Wakai, "Detection of Boron Segregation to Grain Boundaries in Silicon Carbide by Spatially Resolved Electron Energy-Loss Spectroscopy," *J. Am. Ceram. Soc.*, **82** [2], 469-472 (1999).

[58]G. Gouadec, S. Karlin, J. Wu, M. Parlier and Ph. Colomban, "Chemical Physics and Mechanical Imaging of Ceramic Fibres Reinforced Ceramic or Metal Matrix Composites," *Comp. Sci. Techn.* (Special issue on the JNC-11 meeting, Arcachon, France, Nov 98) (2000).

[59]S. Nakashima, H. Katahama, Y. Nakakura and A. Mitsuishi, "Relative Raman Intensities of the Folded Modes in SiC Polytypes," *Phys. Rev.*, **B33** [8], 5721-5729 (1986).

[60]D.W. Feldman, J.H.Parker, W.J. Choyke and L. Patrick, "Phonon Dispersion Curves by Raman Scattering in SiC, Polytypes 3C, 4H, 6H, 15R and 21R," *Phys. Rev.*, **173** [3], 787-793 (1968).

[61]D.W. Feldman, J.H. Parker, W.J. Choyke and L. Patrick, "Raman Scattering in 6H-SiC," *Phys. Rev.*, **170** [3], 698-704 (1968).

[62]I.V. Aleksandrov, A.F. Goncharov, E.V. Yakovenko and S.M. Stishov, "High Pressure Study of Diamond, Graphite and Related Materials," in *High-Pressure Research: Application to Earth and Planetary Sciences*, Y. Syono and M.H. Manghnani Editors, Terra Scientific Publishing Company (TERRAPUB), Tokyo and Am. Geophysical Union, Washington D.C.; pp 409--416 (1992).

[63]S.-I. Nakashima, Y. Nakakura and I. Zenzaburo, "Structural Identification of SiC Polytypes by Raman Scattering : 27R and 33R Polytypes.," *J. Phys. Soc. Jap.*, **56** [1], 359-364 (1987).

[64]S. Nakashima and M. Hangyo, "Raman Intensity Profiles and the Stacking Structure in SiC Polytypes," *Solid State Comm.*, **80** [1], 21-24 (1991).

[65]T. Lopez, E. Haro-Poniatowski, P. Bosh, M. Asomoza, R. Gomez, M. Massot and M. Balkanski, "Spectroscopic Characterization of Lithium Doped Borate Glasses," *J. Sol-Gel Sci. Techn.*, **2**, 891-894 (1994).

[66]G. Gouadec and Ph. Colomban, "Micro-Raman Stress Imaging of Ceramic (C, SiC) Fiber-Reinforced CMCs and MMCs.," *Mater. Sci. Eng. A* (2000).

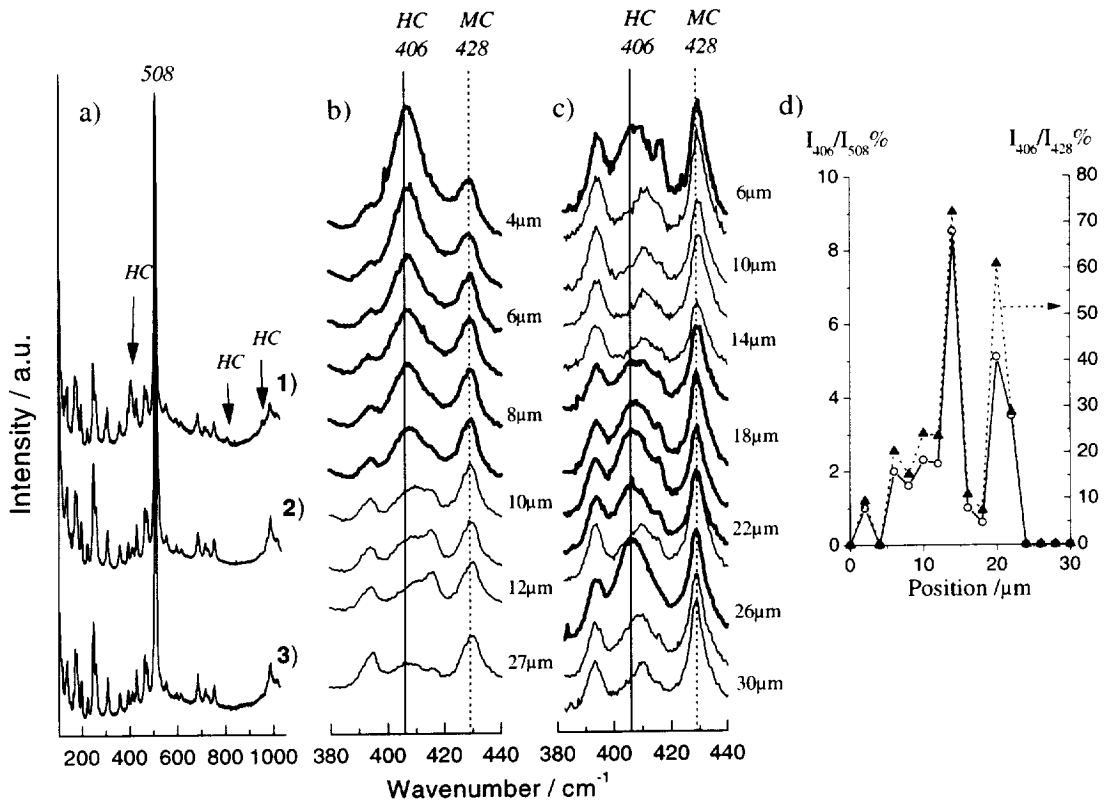

Figure 1: (**a**) Celsian spectra recorded with a mobile mirror scanning the laser along 50 μm lines on the samples section (λ = 488nm, ϕ_{spot} = 1 μm, P = 4 mW): *(1)* unpolished monolith (recording time = 2700s) *(2)* polished composite #1 (2700s) *(3)* unpolished composite #2 (coated fibers, 1800s). All peaks except those with a HC label correspond to the MC phase; (**b**) Spectra recorded "in line" on composite #1 surface, as a function of the distance to the closest fiber (labels) - λ =458nm, P = 4.5 mW, t = 1800 s, slit = 120 μm; spectra in bold have a significant HC contribution; (**c**) Spectra recorded "in line" on composite #2 surface, as a function of the distance to the closest fiber (labels) - λ = 514.5 nm, P = 6 mW, t = 2700s, slit = 75 μm; (**d**) Comparison of the ratios I_{406}/I_{508} (circles) and I_{406}/I_{428} (triangles) calculated after fitting from a mapping between two fibers of composite #2 (λ = 647 nm, step = 2 μm, P = 7 mW, t = 1200 s); Zero means no HC is detected.

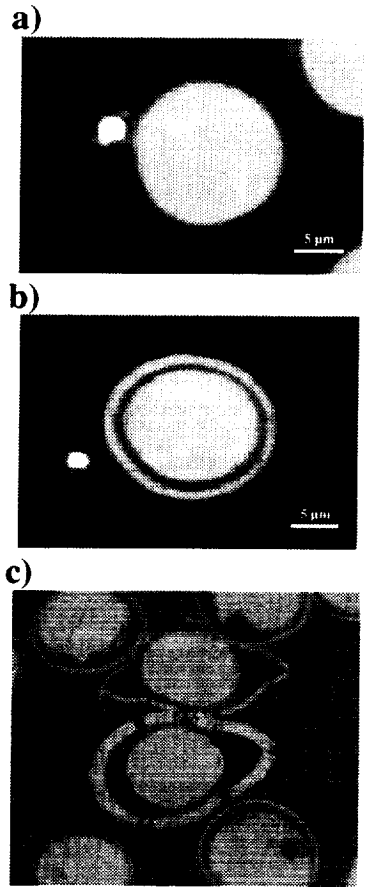

Figure 2 - Optical micrographs of representative fibers (average diameter = 13 μm) in composite #2: **(a)** No visible SiC layer; **(b)** "Thick" SiC layer; **(c)** Broken SiC layer; The white spots in (a) and (b) are laser impacts.

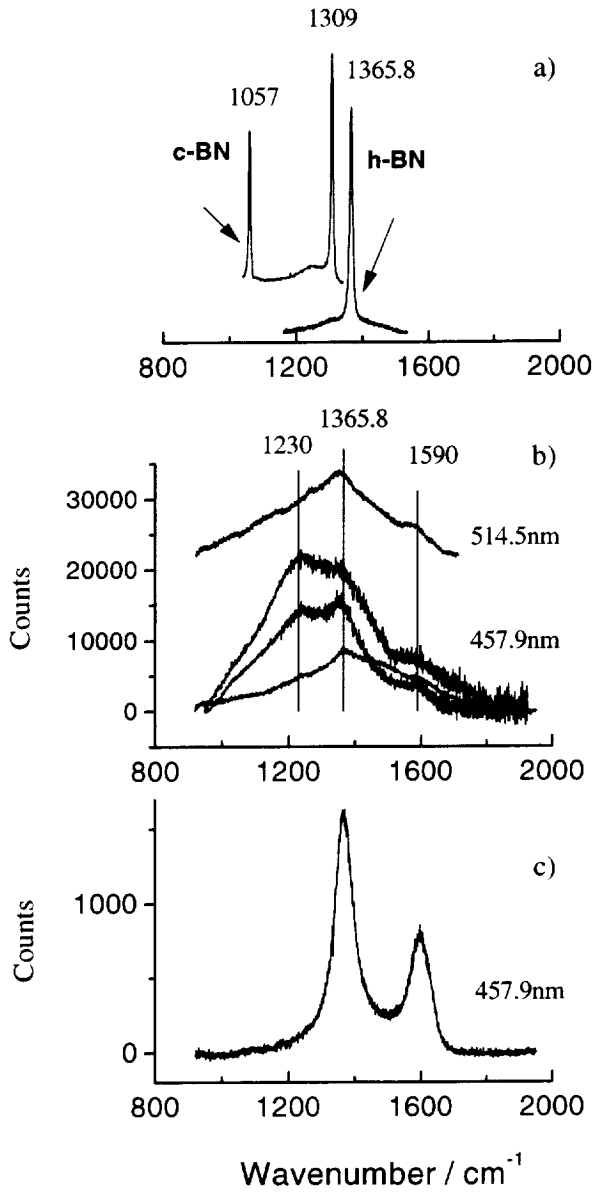

Figure 3: (a) Spectra of the cubic and hexagonal forms of BN. h-BN spectrum (632.8 nm) is from a ceramic grade powder (Herman Starck, Berlin, Germany). c-BN spectrum is reproduced after Werninghaus *et al*[18] (1mm thick single crystal, blue laser). (b) BN spectra recorded on composite #2 (c) one Hi-Nicalon fiber "core spectrum" recorded in the same spectral domain.

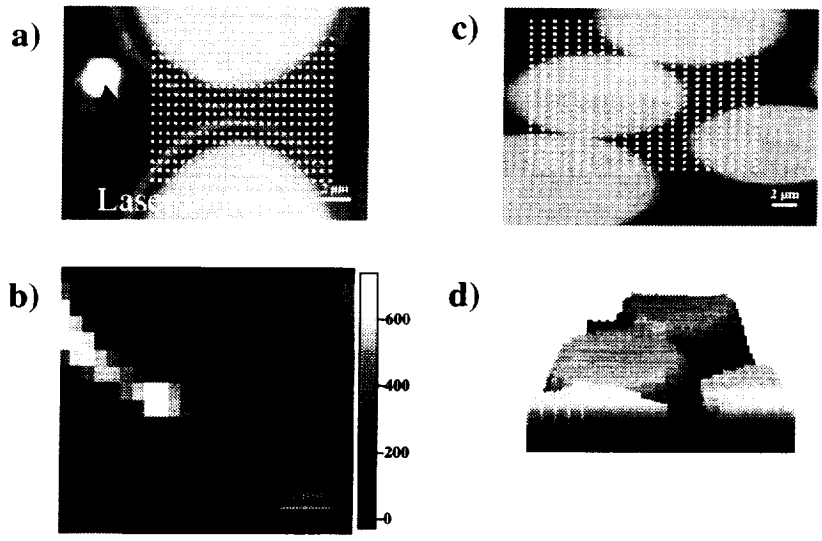

Figure 4 - **(a)** Optical micrograph of a composite #2 polished section; **(b)** The corresponding map is related to the area of spectra recorded for all white dots from 994 to 1784 cm^{-1} (λ = 514.5 nm, P = 2 mW, t = 1 s); **(c)** Optical micrograph of a composite #1 polished section; **(d)** The corresponding map is related to the area in the 1250 - 1450 cm^{-1} range (carbon "D" band; see text) on spectra recorded for all white dots (λ = 514.5 nm, P = 2 mW, t = 90s).

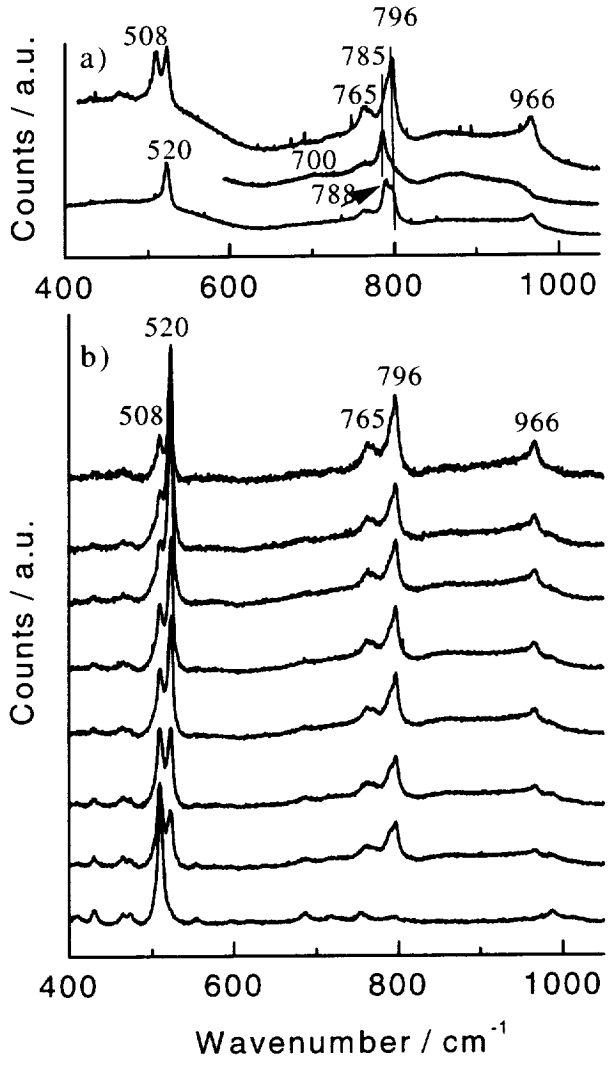

Figure 5: (a) Spectra of SiC rings in composite #2 with λ = 514.5 nm, P = 2 mW (up: 1 hour; down: 900s) and λ = 647 nm (intermediate: 5mW, 900s) (**b**) Spectra recorded in composite #2 (λ = 514.5 nm, P = 2 mW, t = 1200s) from a BN/SiC interface (top) to the celsian matrix (bottom). The step between consecutive spectra is 1µm, but corresponds to 0.25 µm across the SiC layer thickness (see text).

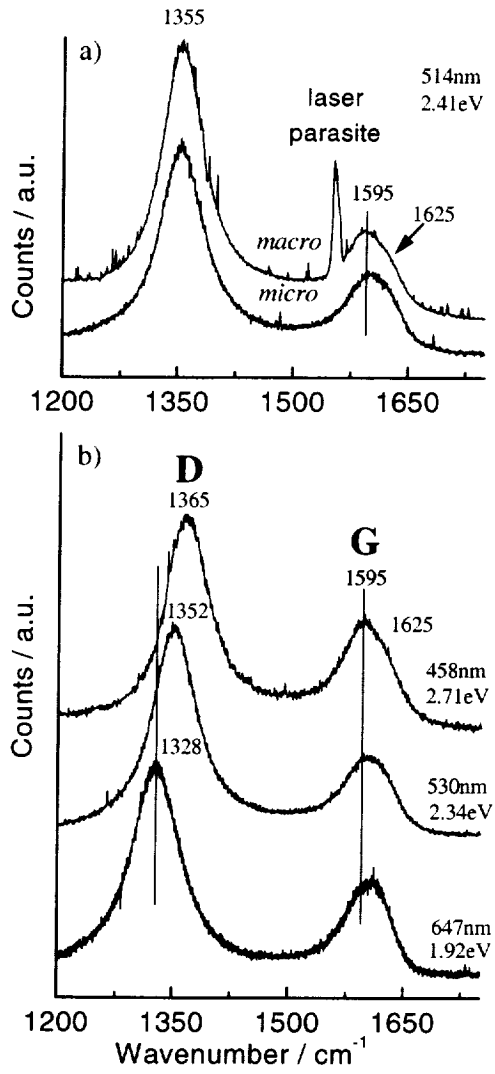

Figure 6: (a) Comparison of spectra recorded on composite #1 in "micro" (single fiber examination) and "macro" (multi-fiber examination)-configurations with the 514.5 nm line (b) Influence of the line on the spectra (1mW, 300s, micro-configuration). Lines are labeled using wavelengths and energy scales: $\varepsilon(eV) \times \lambda(nm) = 1240$.

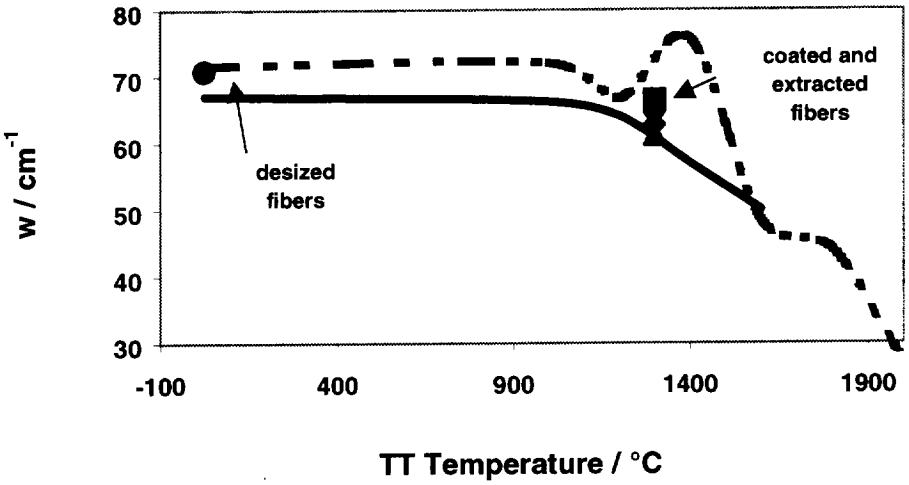

Figure 7: Bandwidth of the "D" peak in free-standing or embedded fibers as a function of the thermal treatment (TT) temperature (λ = 514.5 nm, P = 2 mW). Extracted fibers come from composite #2, dark symbols correspond to composite #1 (lozenge), composite #2 (square) and a composite similar to composite #2 with a 12 wt % Si-doped p-BN layer (triangle). "Reference" curves for annealed non-embedded Hi-Nicalon fibers are reproduced from Ph. Colomban[6] and Gouadec & Colomban[66] (solid = treatment in air; dots = reducing atmosphere).

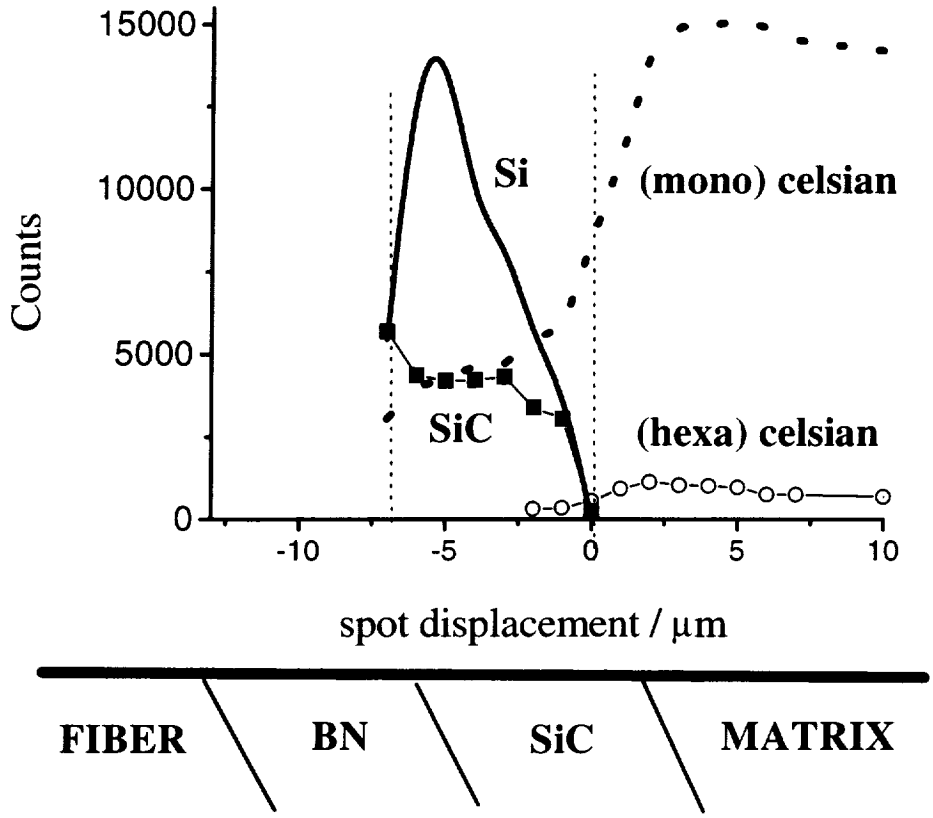

Figure 8: Absolute intensities of the peaks detected on composite #2 mapping of figure 5(b) (λ = 514.5 nm, P = 2 mW, t = 1200s). The sample had been polished with an approximate 15° angle between the fiber plies and the surface so that the "apparent" interphase thickness is almost 4 times greater than the "true" one.

REPORT DOCUMENTATION PAGE

Form Approved
OMB No. 0704-0188

1. AGENCY USE ONLY (*Leave blank*)	2. REPORT DATE	3. REPORT TYPE AND DATES COVERED
	August 2000	Technical Memorandum

4. TITLE AND SUBTITLE

Raman Study of Uncoated and p-BN/SiC-Coated Hi-Nicalon Fiber-Reinforced Celsian Matrix Composites

Part 1: Distribution and Nanostructure of Different Phases

5. FUNDING NUMBERS

WU-523-31-13-00

6. AUTHOR(S)

Gwénaël Gouadec, Philippe Colomban, and Narottam P. Bansal

7. PERFORMING ORGANIZATION NAME(S) AND ADDRESS(ES)

National Aeronautics and Space Administration
John H. Glenn Research Center at Lewis Field
Cleveland, Ohio 44135-3191

8. PERFORMING ORGANIZATION REPORT NUMBER

E-12398

9. SPONSORING/MONITORING AGENCY NAME(S) AND ADDRESS(ES)

National Aeronautics and Space Administration
Washington, DC 20546-0001

10. SPONSORING/MONITORING AGENCY REPORT NUMBER

NASA TM—2000-210349

11. SUPPLEMENTARY NOTES

Gwénaël Gouadec, Laboratoire Dynamique-Interactions-Réactivité (LADIR), UMR7075 - CNRS & Université Pierre et Marie Curie, Thiais, Val de Marne, 94320, France and Département Matériaux & Systèmes Composites (DMSC), Office National d'Etudes et de Recherches Aérospatiales (ONERA), Chatillon, Hauts de Seine, 92322, France; Philippe Colomban, Laboratoire Dynamique-Interactions-Réactivité (LADIR), UMR7075 - CNRS & Université Pierre et Marie Curie, Thiais, Val de Marne, 94320, France; and Narottam P. Bansal, NASA Glenn Research Center. Responsible person, Narottam P. Bansal, organization code 5130, (216) 433-3855.

12a. DISTRIBUTION/AVAILABILITY STATEMENT

Unclassified - Unlimited
Subject Category: 24 Distribution: Nonstandard

This publication is available from the NASA Center for AeroSpace Information, (301) 621-0390.

12b. DISTRIBUTION CODE

13. ABSTRACT ***(Maximum 200 words)***

Hi-Nicalon fiber reinforced celsian matrix composites were characterized by Raman spectroscopy and imaging, using several laser wavelengths. Composite #1 is reinforced by as-received fibers while coatings of p-BN and SiC protect the fibers in composite #2. The matrix contains traces of the hexagonal phase of celsian, which is concentrated in the neighborhood of fibers in composite #1. Some free silicon was evident in the coating of composite #2 which might involve a {BN + SiC → BNC + Si} "reaction" at the p-BN/SiC interface. Careful analysis of C-C peaks revealed no abnormal degradation of the fiber core in the composites.

14. SUBJECT TERMS

Celsian; Composites; Raman spectroscopy; Ceramics

15. NUMBER OF PAGES

26

16. PRICE CODE

A03

17. SECURITY CLASSIFICATION OF REPORT	18. SECURITY CLASSIFICATION OF THIS PAGE	19. SECURITY CLASSIFICATION OF ABSTRACT	20. LIMITATION OF ABSTRACT
Unclassified	Unclassified	Unclassified	